Journal of Hazardous Materials 168 (2009) 1239–1245

Contents lists available at ScienceDirect

Journal of Hazardous Materials

journal homepage: www.elsevier.com/locate/jhazmat

Application of chemometrics methods for the simultaneous kinetic spectrophotometric determination of aminocarb and carbaryl in vegetable and water samples

Yongnian Ni[a,b,*], Weiqiang Xiao[b], Serge Kokot[c]

[a] State Key Laboratory of Food Science and Technology, Nanchang University, Nanchang, Jiangxi 330047, China
[b] Department of Chemistry, Nanchang University, Nanchang, Jiangxi 330047, China
[c] Inorganic Materials Research Program, School of Physical and Chemical Sciences, Queensland University of Technology, Brisbane, Queensland 4001, Australia

ARTICLE INFO

Article history:
Received 30 October 2008
Received in revised form 15 January 2009
Accepted 2 March 2009
Available online 13 March 2009

Keywords:
Spectrophotometry
Aminocarb
Carbaryl
Chemometrics
Differential kinetic method

ABSTRACT

A procedure for the simultaneous kinetic spectrophotometric determination of aminocarb and carbaryl in vegetable and water samples was described. The method was based on the differential oxidation rate of aminocarb and carbaryl when they were reacted with the oxidant, potassium ferricyanide ($K_3Fe(CN)_6$), in an appropriate alkaline medium. Both species were instantly oxidized, and resulted in a decrease of ferricyanide concentration. This anion has a maximum spectral absorbance at about 420 nm. Under the optimum experimental conditions, the linear ranges were 0.05–0.6 mg L^{-1} and 0.1–1.2 mg L^{-1} for aminocarb and carbaryl, respectively. The kinetic data collected were processed by chemometrics methods, such as classical least squares (CLS), partial least squares (PLS), principal components regression (PCR), back propagation-artificial neural network (BP-ANN), radial basis function-artificial neural network (RBF-ANN), and principal component-radial basis function-artificial neural network (PC-RBF-ANN). These methods were applied for the prediction of the two carbamate pesticides. The results showed that the PLS and PC-RBF-ANN calibration models gave the lowest prediction errors. The proposed method was successfully applied to the simultaneous determination of aminocarb and carbaryl in vegetable and water samples, and satisfactory results were obtained.

1. Introduction

Modern pesticides, such as the nonpersistent N-methyl and carbamoyloxime carbamates have replaced the organochlorine and organophosphorus compounds, and are used in large amounts for both agricultural and non-agricultural purposes. They have a broad action spectrum, are highly effective, and generally, have low mammalian toxicity. Their applications as insecticides, fungicides, or herbicides are related to their molecular structure (Table 1), and as insecticides they typically possess the N-substituted carbamate moiety and an aromatic ester or oxime group [1,2]. In addition, their toxicity relates to their ability to act as cholinesterase inhibitors and to form potential mutagens such as N-nitrosocarbamates. Carbamate insecticides such as aminocarb (4-dimethylamino-3-methyl-N-carbamate) and carbaryl (1-naphthyl-N-methylcarbamate) are toxic to humans. However, they are widely used in agriculture to treat stored grain, grass lawns, fruits and vegetables in order to control a number of insect pests such as Lepidoptera and Coleoptera [3–5]. Thus, these pesticides and their degradation products remain as contaminants in environmental samples, such as soil, groundwater, surface water, and also in food. There are many analytical methods for the determination of aminocarb [6–9] and carbaryl [10–14] in waters or vegetables. Although many of these methods are suitable, they are time-consuming and require relatively expensive instrumentation, and some toxic organic reagents. Therefore, simple, sensitive, and reliable alternative methods would be advantageous and useful. Such a possible alternative approach could be based on the differential kinetic spectrophotometric analysis of these two compounds. The principles and applications of the differential kinetic methods have been previously summarized [15,16]. They involve either a reaction with a common reagent or a passage through a common chemical process. Differences in the reaction or process kinetics are used to distinguish the analytes without the need for physical separation. The major limitation of many conventional techniques for processing kinetic data is their reliance on an accurate kinetics model of the system under study. This requires knowledge of the reaction order and rate constants of each reaction in the chemical system. In general, continuing work on handling kinetic data with chemometrics techniques suggests that perhaps the most

* Corresponding author at: Department of Chemistry, Nanchang University, East Nanjing Rd., Nanchang, Jiangxi 330047, China. Tel.: +86 791 3969500; fax: +86 791 3969500.
E-mail address: ynni@ncu.edu.cn (Y. Ni).

0304-3894/$ – see front matter © 2009 Elsevier B.V. All rights reserved.
doi:10.1016/j.jhazmat.2009.03.003

Table 1
Chemical structures of aminocarb and carbaryl.

Pharmaceuticals	Molecular formula	Molecular weight	Chemical structures
Aminocarb	$C_{11}H_{16}N_2O_2$	208.26	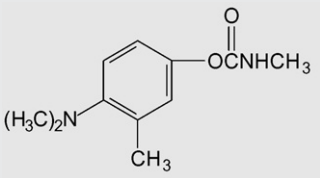
Carbaryl	$C_{12}H_{11}NO_2$	201.22	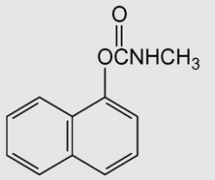

useful models are those which do not need an assumed kinetic model. In particular, recent publications [17–19] involving multivariate calibration methods have successfully demonstrated the use of classical least squares (CLS), principal component regression (PCR), partial least squares regression (PLS), back propagation-artificial neural network (BP-ANN), radial basis function-artificial neural network (RBF-ANN), and principal component-radial basis function-artificial neural network (PC-RBF-ANN).

In this paper, we report the research and development of a differential kinetic spectrophotometric method for the simultaneous determination of the two carbamate pesticides, aminocarb and carbaryl, with the aid of chemometrics. The method was based on the different kinetics of these two substances, when they reacted with potassium ferricyanide in an appropriate alkaline medium. The kinetic data collected was processed by several chemometrics methods to develop the calibration models, and these methods were then validated with the aid of synthetic samples containing mixtures of the two compounds. Thereafter, the best performing methods were applied to analyse several vegetable and water samples to demonstrate their general applicability.

2. Methodology

2.1. Kinetic models

Consider that two analytes, A and B, react with a common reagent, R, to give the same absorbing product P, according to the following scheme:

$$A + R \rightarrow P_A \quad (1)$$

$$B + R \rightarrow P_B \quad (2)$$

where P_A and P_B correspond to the products obtained from A and B, respectively. If it is assumed that the two reactions involved follow first or pseudo first-order kinetics with respect to the concentration of the analytes, the rate equations for A and B are:

$$-\frac{dc_A}{dt} = k_A c_A \quad (3)$$

$$-\frac{dc_B}{dt} = k_B c_B \quad (4)$$

where c_A and c_B are the concentrations of A and B at time, t, and k_A and k_B are the rate constants of A and B.

Integration of Eqs. (3) and (4) yields:

$$c_A = c_{A,0}\exp(-k_A t) \quad (5)$$

$$c_B = c_{B,0}\exp(-k_B t) \quad (6)$$

where $c_{A,0}$ and $c_{B,0}$ are the initial concentration of A and B. According to the stoichiometric factors between the analytes and products, the concentrations of P_A and P_B at time, t, can be represented as follows:

$$c_{PA} = c_{A,0}[1 - \exp(-k_A t)] \quad (7)$$

$$c_{PB} = c_{B,0}[1 - \exp(-k_B t)] \quad (8)$$

where c_{PA} and c_{PB} represent the concentrations of P_A and P_B at time, t, during the reaction process, respectively.

If it is assumed that the two analytes behave independently and their absorbances are additive, then the absorbance of the mixture of A and B may be written as

$$\begin{aligned} A &= A_{P_A} + A_{P_B} \\ &= \varepsilon_A b c_{P_A} + \varepsilon_{P_B} b c_{P_B} \\ &= c_{A,0}\varepsilon_{P_A} b[1 - \exp(-k_A t)] + c_{B,0}\varepsilon_{P_B} b[1 - \exp(-k_B t)] \\ &= K_A c_{A,0} + K_B c_{B,0} \end{aligned} \quad (9)$$

where ε_{P_A} and ε_{P_B} are absorptivity of P_A or P_B, respectively, K_A and K_B are proportional coefficients for component A and B, respectively, and b is the optical cell length.

If m standard samples are prepared, the absorbance data of kinetic systems being monitored at time, s, can be expressed in matrix form as follows:

$$\boldsymbol{A}_{m\times s} = \boldsymbol{C}_{m\times 2}\boldsymbol{K}_{2\times s} \quad (10)$$

The data matrix, $\boldsymbol{A}_{m\times s}$, may be used to determine the concentration of the pesticide analytes simultaneously with the use of a suitable chemometrics method such as CLS, PCR, PLS, BP-ANN, RBF-ANN, and PC-RBF-ANN.

2.2. Multivariate calibration and artificial neural network methods

2.2.1. Classical least squares method

CLS [20] is a very common multivariate calibration method and has been used for quantitative spectral analysis. This method is generally based on the assumption that there is a linear relationship between the response signals and the concentrations of the analytes. In addition, this method requires a calibration step where the relationship between the spectra and component concentrations is estimated from a set of standard samples. This step is followed by prediction in which the calibration model is used to estimate the concentrations of the components from the spectra of unknown samples. A major disadvantage of CLS is that all interfering chemical components in the spectral region of interest need to be included in the calibration models.

2.2.2. Principal component regression and partial least squares methods

PCR [21] and PLS [22] are factor analysis-based multivariate statistical tools, which have many of the full-spectrum advantages of the CLS method, and have been successfully applied for the analysis of multicomponent mixtures. As with the CLS method, PCR and PLS methods require a calibration step, which is followed by a prediction step for the estimation of the concentrations in the unknown samples. Both of these methods involve spectral decomposition. The PCR decomposition is based entirely on spectral variations without regard for the component concentrations, and in PLS, the spectral decomposition is weighted to the concentration matrix.

2.2.3. Back-propagation artificial neural network method

BP-ANN is sometimes called the multilayer feed forward (MLF) networks method, and is a popular neural network approach. Its basic theory and application to chemical problems have been discussed elsewhere [23,24]. This model is composed of a large number of simple processing elements or neuron nodes which are organized into a sequence of layers. The first layer is the input layer with one node for each variable of the data. The second layer is the hidden layer consisting of a number of nodes, which are used for learning. The last layer is the output layer consisting of one node for each variable in the matrix. Nodes in any layer are fully or randomly connected to nodes of a succeeding layer. During the training process, each connection between the nodes of different layers is represented by a weight, ω_{ij}, which is defined as

$$\Delta\omega_{ij(n+1)} = \Delta\eta\delta_j o_j + \alpha\Delta\omega_{ij(n)} \tag{11}$$

where δ_j is the error term, o_j the output of node j, η the learning rate, α the momentum, and n is the iteration number. Iteration is completed when the error of prediction reaches a minimum. In this work, a non-linear sigmoidal transfer function was applied between the input and output of node, and the concentration values were scaled from 0.2 to 0.8 by multiplying by a constant to accommodate the bounded range of the function output. Optimal values of η and α were taken as those with minimized error of prediction. In BP networks, supervised training approach is used to optimize the proper setting of the weights. In general, the weights are optimized with the use of some training input samples together with their associated desired outputs. The weight updates are based on the difference between the actual and the desired output of the network. The weight updating can be carried out after each sample or it can be done after all training samples have been processed. The two procedures are strictly equivalent.

2.2.4. Principal component-radial basis function-artificial neural network methods

RBF-ANN architecture is similar to that of BP-ANN. It offers some advantages over the BP-ANN by improving the robustness and sensitivity of the model when dealing with noisy data. Its basic theory and application to chemical problems have been reported in the literature [25–27]. Its model also involves three layers. The first layer is made up of input nodes that transmit unweighted inputs to each node in the hidden layer. Each hidden node contains a radial basis function as the transfer function. The outputs of these nodes are weighted and summed to produce the final output. In contrast to the sigmoid function, the kernel or basis function is classified as a local activation function. The main difference between the transfer function in the BP networks and the kernel function in the RBF networks, is that the latter (usually a Gaussian function) defines an ellipsoid in the input space. The key to a successful implementation of the RBF networks is to find suitable a centre for such a Gaussian function, which is characterized by two parameters, i.e. centre (c_j), and peak width (σ_j). The output from the jth Gaussian neuron for an input object, x_i, can be calculated by the following equation:

$$\text{output}_j = o_j(x) = \exp\left(\frac{-|x_i - c_j|^2}{\sigma_j}\right) \tag{12}$$

where $|x_i - c_j|$ is the calculated Euclidean distance between x_i, and c_j, and σ_j determines the portion of the input space where the jth RBF will have a non-significant zero response. After selection of the centre and peak width, the connections between the radial basis units and the output node are weighted. The output of the net is consequently given by

$$y_i = \sum_{i=1}^{n} \omega_{ji} o_j(x) \tag{13}$$

where ω_{ji} represents the weights of the connections between the hidden layer, i, and output layer, j, and $o_j(x)$ is obtained from Eq. (12).

PC-RBF-ANN is an improved RBF-ANN model, which has been successfully applied for the determination of analytes in mixtures [17,18]. In this method, the kinetics data of the calibration mixtures has been previously compressed into scores with the use of PCA, and then the scores of this model were employed as input data to the network. This reduced considerably the ANN-training time without loss of information.

3. Experimental

3.1. Apparatus

Spectra were measured on an Agilent 8453 UV–vis spectrophotometer equipped with a Model ZC-10 thermostat temperature control accessory (Ningbo Tianhe Instruments Factory, China). These measurements were made with the use of a 10 mm path-length fused-silica cell. The sample solutions were subjected to a short sonication (SK1200H, Kudos Ultrasonic Instrument Co. Ltd., Shanghai), and all solution volumes of less than 1 mL were delivered with micropipettes (Finnpipette, Labsystems, Finland). The obtained data were processed on a Pentium IV computer with programs written in MATLAB 6.5 (Math works).

3.2. Solutions and reagents

All solutions were prepared with Analytical Grade reagents, and doubly distilled water was used throughout. Stock solutions of aminocarb and carbaryl (100.0 mg L^{-1}) were prepared from suitable weight aliquots, and dissolved with 20 mL methanol in a 100 mL volume flask. The solution was then diluted to the mark with distilled water and mixed well. Stock solutions of potassium ferricyanide ($K_3Fe(CN)_6$, 2.0×10^{-4} mol L^{-1}) and sodium hydroxide (2.0 mol L^{-1}) were prepared by taking suitable weight aliquots of the reagents and dissolving them in water. The standard solutions were stored in a refrigerator and protected from light.

3.3. General procedure

For spectrophotometric analysis, the analytes and any other reagents were added directly into the 10 mm cell by using micropipettes (ThermoLabsystems). Taking into account that the total useful volume was 2.5 mL, x mL of the analyte solution, 0.4 mL sodium hydroxide solution were added to the cell, followed by $(1.85 - x)$ mL doubly distilled water to give a volume of 2.25 mL. The cell was shaken and left to stand for 90 s in the temperature-controlled holder of the spectrophotometer (70 °C) before the absorbance was set to zero. Then 0.25 mL of potassium ferricyanide

was added to the cell as quickly as possible, to give the final volume of 2.5 mL just as the reaction commenced. The absorbance data of this solution was recorded at 420 nm every 2 s between 5 and 240 s with respect to the distilled water blank. Each reagent was added carefully to keep the experimental results consistent and reproducible within the error of the micropipettes, i.e. ~±0.1–1.5 μL and the relative error introduced was less than 1%.

3.4. Procedure for the determination of the carbamates in vegetable samples

Samples of commercial vegetables were homogenized in a blender; then a 10.0 g weight aliquot of this sample was transferred to a 100 mL Erlenmeyer flask (with a screw cap), and 20 mL of dichloromethane (CH_2Cl_2) were added. Because the concentration of pesticides in vegetable samples was too low for direct detection, 2.0 mL of each of the standard solutions of the pesticides were added. Additionally, 5.0 g anhydrous sodium sulfate (Na_2SO_4) was placed into the flask to absorb the water in the sample. The mixture was shaken for 30 min on a Model HY-4 oscillator (Shanghai Instrumental Manufacture, Shanghai), and filtered on a Buchner funnel; the residue in the funnel was further washed with 5 mL of dichloromethane. The filtrate was treated and separated with hexane–acetonitrile (1:1) in a separation funnel; the carbamates were extracted into the acetonitrile phase because of their higher polarity, while the colorants and impurities were extracted into the hexane phase. The acetonitrile phase was treated twice with hexane to extract any residual impurities, and the acetonitrile phase, collected in an evaporating dish, was evaporated to near dryness. Finally, the residue in the evaporating dish was dissolved in ethanol, transferred to a 10 mL volumetric flask and diluted to the mark with 50% ethanol.

3.5. Procedure for the determination of the carbamates in water samples

A water sample was spiked with 2.0 mL of each pesticide from the 100 mg L^{-1} stock solutions. After filtering, the filtrate was transferred into a 100 mL Erlenmeyer flask (with a screw cap), and 1 g of anhydrous sodium sulfate and 25 mL of dichloromethane were added. The mixture was then shaken for 30 min on a Model HY-4 oscillator. The collected aqueous phase was extracted with another 25 mL dichloromethane. The extracts were combined, transferred into an evaporating dish, and evaporated to near dryness. Finally, the residue in the evaporating dish was dissolved in ethanol, transferred to a 10 mL volumetric flask, and diluted to the mark with distilled water.

4. Results and discussion

4.1. Spectra and reaction kinetics

The absorption spectra of aminocarb and carbaryl in aqueous solution overlapped strongly (Fig. 1), and also, showed a weak absorption peak in the UV region. This indicated that simultaneous determination of the analytes by conventional spectral analysis could not produce reliable results. However, the reaction of the two carbamate pesticides with $K_3Fe(CN)_6$ when followed as a function of time (Fig. 2), showed that the carbaryl analyte has a comparatively lower absorbance than the aminocarb. This indicated that the carboryl reaction has a higher rate than the aminocarb one. This observed difference in the kinetic behaviour of the two carbamate pesticides enabled the development of a differential kinetic spectrophotometric analytical method with the aid of chemometrics. The rate constants for the reactions involving aminocarb and carbaryl were estimated by fitting the experimental kinetics data from

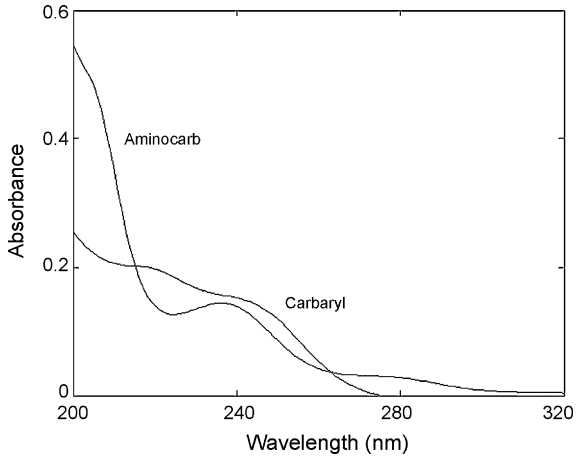

Fig. 1. Absorption spectra of aminocarb (2 mg L^{-1}) and carbaryl (2 mg L^{-1}) in aqueous solution.

single component samples to the equation of $A = a_0 - a_1\exp(-kt)$ by a suitable regression method [28]. Their values were 0.0060 and 0.0095, respectively, giving a relatively low carboryl/aminocarb ratio of 1.5. This indicated a similar reaction behaviour and supported the view that it is difficult to resolve these substances in a mixture by classical differential kinetic methods, such as the logarithmic extrapolation and the proportional equation [16].

4.2. Optimization of the reaction conditions and univariate calibration

The effects of the concentrations of potassium ferricyanide and sodium hydroxide, as well as the temperature on the determination of aminocarb or carbaryl were investigated and the optimum values were found to be 2.0×10^{-4} mol L^{-1}, 0.32 mol L^{-1} and 70 °C, respectively. The absorption maximum of $K_3Fe(CN)_6$ spectrum at 420 nm was selected as the analytical wavelength. The concentration of $K_3Fe(CN)_6$ had to be maintained at a high level (generally, 100 times higher than that of the analytes) to ensure that the pseudo first-order reaction prevailed. However, high concentrations of $K_3Fe(CN)_6$ could give rise to increased spectral backgrounds, and hence, the initial concentration of this complex salt was selected to be 2.0×10^{-4} mol L^{-1} $K_3Fe(CN)_6$. This apparently low value was based on experimental spectral results

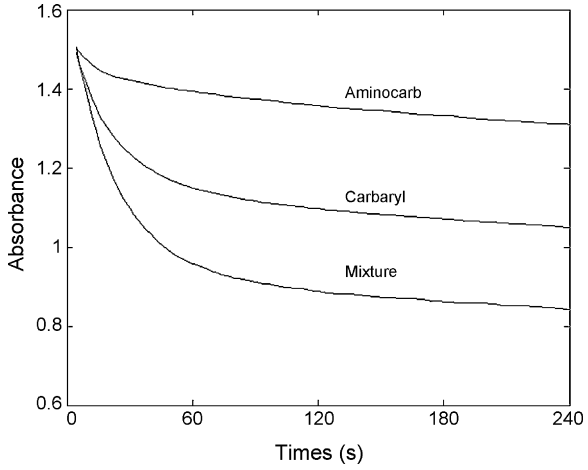

Fig. 2. Absorbance versus time plot for aminocarb (0.15 mg L^{-1}) and carbaryl (0.65 mg L^{-1}) with a total time of 240 s at λ = 420 nm. T = 70 °C, c_{NaOH} = 0.32 mol L^{-1}, and $c_{K_3Fe(CN)_6} = 2.0 \times 10^{-4}$ mol L^{-1}.

Table 2
Comparison of analytical figures of merit for the determination of aminocarb and carbaryl.

Parameter	Aminocarb	Carbaryl
Number of Sample (n)	7	7
Linear range (mg L^{-1})	0.05–0.6	0.1–1.2
Correlation coefficient	0.9999	0.9998
Intercept	1.6	1.4
Slope (L mg^{-1})	−1.8	−0.66
$s_{Intercept}$ ($\times 10^{-4}$)[a]	2.2	3.3
s_{slope} ($\times 10^{-4}$)[a]	5.9	2.4
$s_{Regression}$ ($\times 10^{-3}$)[a]	3.0	3.5
LOD (mg L^{-1})[b]	0.02	0.04

[a] $s_{Intercept}$, s_{slope} and $s_{Regression}$ are the standard deviations of the intercept, the slope and the regression, respectively.

[b] LOD is the limit of detection and was calculated according to Miller and Miller's method [29].

[17], and indicated that the concentrations of the carbamates were to be in the order of 10^{-5} to 10^{-7} mol L^{-1}. Thus, because of the low levels of the analytes, the reaction process was slow. Under these conditions, calibration sets with different concentrations of aminocarb and carbaryl were prepared and absorbance versus time was measured at 420 nm (Table 2 and Fig. 3). The linear concentration ranges for aminocarb and carbaryl were 0.05–0.6 mg L^{-1} and 0.1–1.2 mg L^{-1}, respectively, and their LOD values are 0.02 and 0.04 mg L^{-1} [29]. There was a good linear correlation between the measured absorbance and concentration.

4.3. Simultaneous prediction of aminocarb and carbaryl in a synthetic mixture

For quantitative analysis of the binary mixtures of aminocarb and carbaryl, a set of 11 samples (Fig. 4) was prepared according to the orthogonal array design [30,31] and calibration models were constructed with the aid of the following chemometrics methods: CLS, PCR, PLS, BP-ANN, RBF-ANN and PC-RBF-ANN. These models were validated against another set of nine samples (Fig. 4). Relative prediction errors (RPE) [32] from the calibration models were estimated from the expressions below:

i. RPE for a single component in the mixtures:

$$\%\mathrm{RPE_S} = \left[\frac{\sum_{i=1}^{n}(c_{ij(\mathrm{found})} - c_{ij(\mathrm{added})})^2}{\sum_{i=1}^{n}(c_{ij(\mathrm{added})})^2}\right]^{0.5} \quad (14)$$

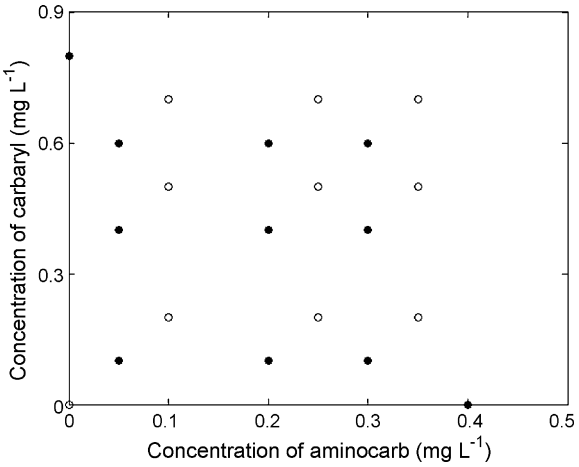

Fig. 4. Composition of the calibration and validation samples. Calibration samples (●) and validation samples (○).

Table 3
Prediction results of aminocarb and carbaryl in validation mixtures by different chemometric methods.

Chemometric methods	%RPE$_S$		%RPE$_T$
	Aminocarb	Carbaryl	Saccharin sodium
CLS	8.9(105)[a]	8.2(99)	8.3
PCR(3)[b]	5.6(102)	5.0(99)	5.2
PLS(3)[b]	5.4(99)	4.9(101)	5.0
BP-ANN(0.05, 0.2, 6, 800)[c]	6.2(103)	5.9(98)	6.0
RBF-ANN(5, 450)[d]	5.3(101)	5.0(102)	5.1
PC-RBF-ANN(3, 5, 300)[e]	5.0(97)	4.6(103)	4.8

The values in the parentheses correspond to:

[a] The mean % recoveries.

[b] The number of factors used.

[c] The parameters of the learning rate, momentum, nodes in the hidden layer, and the maximum number of epochs to train, respectively; sigmoid and linear transfer functions were used to construct the hidden and output layers in the BP-ANN model, respectively.

[d] The parameters of nodes in the hidden layer and the spread coefficient (sc), respectively; initially, the data matrix was normalised.

[e] The number of factors from the PCA, nodes in the hidden layer and the spread coefficient (sc), respectively; initially, data were normalised, and the resulting matrix was submitted to PCA. The extracted scores matrix was used for the neural network training.

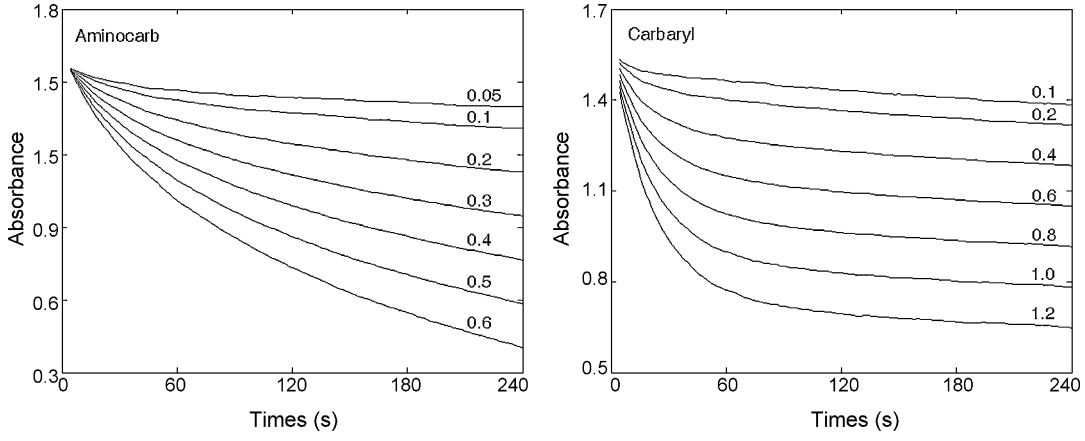

Fig. 3. Kinetic curves for aminocarb and carbaryl with different concentrations (mg L^{-1}). Experimental conditions are as in Fig. 2.

Table 4
Determination of aminocarb and carbaryl in commercial vegetable and water samples by the PLS and PC-RBF-ANN methods (mg L^{-1}).

Samples[a]	Spiked		Found		Recovery (%)	
	Aminocarb	Carbaryl	Aminocarb	Carbaryl	Aminocarb	Carbaryl
PLS[b]						
Spinach	0.400	0.400	0.347	0.352	86.8	88.0
Potato	0.400	0.400	0.342	0.348	85.5	87.0
Tap water	0.400	0.400	0.372	0.378	93.0	94.5
Pond water	0.400	0.400	0.365	0.370	91.3	92.5
Qianhu Lake	0.400	0.400	0.364	0.369	91.0	92.3
PC-RBF-ANN[b]						
Spinach	0.400	0.400	0.350	0.366	87.5	91.5
Potato	0.400	0.400	0.362	0.368	90.5	92.0
Tap water	0.400	0.400	0.344	0.348	86.0	87.0
Pond water	0.400	0.400	0.378	0.380	94.5	95.0
Qianhu Lake	0.400	0.400	0.382	0.379	95.5	94.8

[a] Spinach and potatoes were obtained from a supermarket in Nanchang city; tap water, pond water and the Qianhu Lake water were obtained from the countryside of Nanchang.
[b] Parameters used were as in Table 3.

ii. RPE for the total prediction error:

$$\%\mathrm{RPE}_{\mathrm{T}} = 100 \times \left[\frac{\sum_{i=1}^{n}\sum_{j=1}^{m}(c_{ij(\mathrm{found})} - c_{ij(\mathrm{added})})^2}{\sum_{i=1}^{n}\sum_{j=1}^{m}(c_{ij(\mathrm{added})})^2} \right]^{0.5} \quad (15)$$

where $c_{ij(\mathrm{added})}$ indicates the concentration of component, i, in mixture, j, and $c_{ij(\mathrm{found})}$ is its estimate. n and m are the number of validation samples and the number of analytes to be determined, respectively.

The $\mathrm{RPE}_{\mathrm{S}}$, $\mathrm{RPE}_{\mathrm{T}}$, and the percentage mean recovery for each chemometric method (Table 3) showed that the CLS method produced the worst results—an observation which is in agreement with general experience with such models; the PCR, PLS, RBF-ANN and PC-RBF-ANN gave very similar results at %RPE of about 5, while BP-ANN gave slightly worse %RPE value (~6). This prediction performance of the calibration methods is consistent with previous observations [33]. Mean recoveries for all calibrations were found to be satisfactory in the range of 97–105%.

It is important to note that from a practical point of view of the analyst, all methods apart from the CLS one, would be suitable to employ for calibration purposes. This is important because while PCR and PLS methods are readily available as commercial software, ANN, at present, is somewhat more difficult to obtain and operate. However, for the purposes of this investigation involving the simultaneous prediction of carboryl and aminocarb pesticides, we applied the calibrations from the slightly better performing method, PC-RBF-ANN, and also, for comparison, the commonly used and readily available PLS method.

4.4. Interfering effects

In general, pesticides other than the analytes, carboryl and aminocarb, could have an inhibitory effect on the reaction process, and they could also contribute to spectral absorption to some extent, in the working wavelength range. Thus, the possible interference of some pesticides that are generally used in China was investigated in this study. The determination of aminocarb and carbaryl, both at 0.4 mg L^{-1}, in the presence of these pesticides, was investigated for interference to a level of ±10% $\mathrm{RPE}_{\mathrm{T}}$. The ratio values of the [interferant]/[analyte pesticide] at that level for aminocarb and carbaryl were: 150, isoprocarb; 100, propoxur and carbofuran; 80, chlorpyrifos; 50, methyl-parathion; 40, methamidophos and fenitrothion. It would appear that the interference of many of these pesticides should be relatively minor. However, these results provide only a guide for these potential interferences because the exact quantitative effects need to be checked if the method is applied specifically for the analysis of the two analytes at lower concentrations.

4.5. Analysis of aminocarb and carbaryl in vegetable and water samples

The proposed kinetic-spectrophotometric method was applied for the determination of the aminocarb and carbaryl in two vegetables (spinach, and potatoes) and three water samples (tap water, pond water, and lake water). As the PLS and PC-RBF-ANN calibration models gave the better prediction results, they were applied for the determination of the pesticides in real samples (Table 4). Also reported were the results obtained for standard additions of the pesticide analytes to each sample. The efficacy of the procedure was further confirmed by the %Recovery values in the range of 85.5–95.5. It was noted that there was some loss of the pesticides during the extraction procedure, and the distribution ratios of the analytes in hexane–acetonitrile is about 87.5%. This ratio was considered in the calculation for %Recovery, and the estimated concentration of the analytes was adjusted by 12.5%.

5. Conclusion

An accurate and simple method was researched and developed for the simultaneous determination of aminocarb and carbaryl in the vegetable and water samples. The results showed the successful application of the proposed method to the simultaneous quantification with total relative prediction errors ($\%\mathrm{RPE}_{\mathrm{T}}$) of 5.0 and 4.8 for PLS and PC-RBF-ANN. The method was based on the difference in the oxidation rate of these compounds with yellow potassium ferricyanide in appropriate alkaline medium to form colorless potassium ferrocyanide. The spectral data obtained were processed by calibration models based on different chemometrics methods. The predicted results of validation samples showed that the PLS and PC-RBF-ANN models had distinct advantages over the other chemometrics models. The proposed method was also applied for the simultaneous determination of carbaryl and aminocarb in the vegetable and water samples with satisfactory results.

Acknowledgements

The authors gratefully acknowledge the financial support of this study by the Natural Science Foundation of China (NSFC20562009), the Jiangxi Province Natural Science Foundation (JXNSF0620041),

State Key Laboratory of Food Science and Technology (SKLF-MB200807 and SKLF–TS200819) and the program for Changjiang Scholars and Innovative Research Team in Universities (IRT0540).

References

[1] Y.N. Ni, D.X. Cao, S. Kokot, Simultaneous enzyme kinetic determination of pesticides, carbaryl and phoxim, with the aid of chemometrics, Anal. Chim. Acta 588 (2007) 131–139.
[2] M. Hashimoto, A. Mizutani, K. Tago, M. Ohnishi-Kameyama, T. Shimojo, M. Hayatsu, Cloning and nucleotide sequence structure of carbaryl hydrolase gene (cahA) from Arthrobacter sp. RC100, J. Biosci. Bioeng. 101 (2006) 410–414.
[3] G.F. Jia, L. Li, J. Qiu, X.Q. Wang, W.T. Zhu, Y. Sun, Z.Q. Zhou, Determination of carbaryl and its metabolite 1-naphthol in water samples by fluorescence spectrophotometer after anionic surfactant micelle-mediated extraction with sodium dodecylsulfate, Spectrochim. Acta A 67 (2007) 460–464.
[4] K.S. Kumar, K. Suvardhan, P. Chiranjeevi, Preparation of reagents for the sensitive spectrophotometric determination of carbaryl in environmental samples, Anal. Lett. 38 (2005) 697–709.
[5] K.M.S. Sundaram, N. Boyonoski, R.W. Wing, B.L. Cadogan, Simultaneous determination of fenitrothion and aminocarb in blueberry foliage and fruits-application to the analysis of residues in field samples, J. Environ. Sci. Health B 22 (1987) 565–578.
[6] K.M.S. Sundaram, J. Curry, High-performance liquid chromatographic method for the analysis of aminocarb, mexacarbate and some of their N-methylcarbamate metabolites by post-column derivatization with fluorescence detection, J. Chromatogr. A 672 (1994) 117–124.
[7] K.M.S. Sundaram, Liquid-chromatographic method for the determination of nonyl phenol surfactant in the commercial and spray formulations of aminocarb (matacil (R)) insecticide, J. Liq. Chromatogr. 18 (1995) 1787–1799.
[8] K.M.S. Sundaram, J. Curry, Fluorometric-determination of aminocarb and mexacarbate and some of their metabolites by liquid-chromatography influence of structural factors on fluorescence intensity, J. Liq. Chromatogr. 17 (1994) 3759–3774.
[9] S.C. Slachck, Liquid-chromatographic determination of aminocarb in technical and formulated products collaborative study, J. AOAC Int. 68 (1985) 567–569.
[10] F. Koc, Y. Yigit, Y.K. Das, Y. Gurel, C. Yaral, Determination of aldicarb, propoxur, carbofuran, carbaryl and methiocarb residues in honey by HPLC with post-column derivatization and fluorescence detection after elution from a florisil column, J. Food Drug Anal. 16 (2008) 39–45.
[11] A. Waseem, M. Mohammad, A. Nabi, Flow-injection determination of carbaryl and carbofuran based on $KMnO_4$–Na_2SO_3 chemiluminescence detection, Luminescence 22 (2007) 349–354.
[12] S. Totti, M. Fernandez, S. Ghini, Y. Pico, F. Fini, J. Manes, S. Girotti, Application of matrix solid phase dispersion to the determination of imidacloprid, carbaryl, aldicarb, and their main metabolites in honeybees by liquid chromatography–mass spectrometry detection, Talanta 69 (2007) 724–729.
[13] S.S.E. Petropoulou, A. Tsarbopoulos, P.A. Siskos, Determination of carbofuran, carbaryl and their main metabolites in plasma samples of agricultural populations using gas chromatography–tandem mass spectrometry, Anal. Bioanal. Chem. 385 (2006) 1444–1456.
[14] L. Codognoto, S.T. Tanimoto, V.A. Pedrosa, H.B. Suffredini, S.A.S. Machado, L.A. Avaca, Electroanalytical determination of carbaryl in natural waters on boron doped diamond electrode, Electroanalysis 18 (2006) 253–258.
[15] H.A. Mottola, Kinetic Aspects of Analytical Chemistry, Wiley, New York, 1988.
[16] D. Perez-Bendito, M. Silva, Kinetic Methods in Analytical Chemistry, Ellis Horwood, New York, 1988.
[17] Y.N. Ni, C.F. Huang, S. Kokot, A kinetic spectrophotometric method for the determination of ternary mixtures of reducing sugars with the aid of artificial neural networks and multivariate calibration, Anal. Chim. Acta 480 (2003) 53–65.
[18] Y.N. Ni, Y. Wang, Application of chemometrics methods to the simultaneous kinetic spectrophotometric determination of iodate and periodate based on consecutive reactions, Microchem. J. 86 (2007) 216–226.
[19] Y.N. Ni, Y. Wang, S. Kokot, Simultaneous determination of three fluoroquinolones by linear sweep stripping voltammetry with the aid of chemometrics, Talanta 29 (2006) 216–225.
[20] C. Schmidt Peter, W. Glombitza Bernhard, Quantitative multicomponent analysis of aspirin and salicylic acid in tables without separation of excipients by means of principal component regression and a classical least squares algorithm, Trends Anal. Chem. 14 (1995) 45–49.
[21] I.T. Jolliffe, Principal Component Analysis, Springer, New York, 1986.
[22] M. Lipp, Determination of the adulteration of butter fat by its triglyceride composition obtained by GC. A comparison of the suitability of PLS and neural networks, Food Chem. 55 (1996) 389–395.
[23] J. Zupan, J. Gasteiger, Neural Networks for Chemists: An Introduction, VCH, Weinheim, 1993.
[24] A. Afkhami, M. Abbasi-Tarighat, M. Bahram, Artificial neural networks for determination of enantiomeric composition of α-phenylglycine using UV spectra of cyclodextrin host–guest complexes: comparison of feed–forward and radial basis function networks, Talanta 75 (2008) 91–98.
[25] P.J. Braspenning, F. Thuijsman, A.J.M.M. Weijters, Artificial Neural Networks: An Introduction to ANN Theory and Practice (Lecture Notes in Computer Science), Springer, New York, 1995.
[26] M. Hasani, M. Moloudi, Application of principal component-artificial neural network models for simultaneous determination of phenolic compounds by a kinetic spectrophotometric method, J. Hazard. Mater. 157 (2008) 161–169.
[27] M. Chamsaz, A. Safavi, J. Fadaee, Simultaneous kinetic-spectrophotometric determination of carbidopa, levodopa and methyldopa in the presence of citrate with the aid of multivariate calibration and artificial neural networks, Anal. Chim. Acta 603 (2007) 140–146.
[28] N.R. Draper, H. Smith, Applied Regression Analysis, 3rd ed., Wiley, New York, 1998.
[29] J.N. Miller, J.C. Miller, Statistics and Chemometrics for Analytical Chemistry, 4th ed., Pearson Education Limited, London, 2000.
[30] G. Taguchi, System of Experimental Design, vols. 1 and 2, Kraus, New York, 1987.
[31] Y.N. Ni, The Application of Chemometrics in Analytical Chemistry, Chinese Science Press, Beijing, 2004.
[32] M. Otto, W. Wegscheider, Spectrophotometric multicomponent analysis applied to trace metal determinations, Anal. Chem. 57 (1985) 63–69.
[33] Y.N. Ni, Y. Wang, S. Kokot, Simultaneous kinetic-spectrophotometric determination of maltol and ethyl maltol in food samples by using chemometrics, Food Chem. 109 (2008) 431–438.